

# Wrong-Helicity Electrons in Radiative Muon Decay

V. S. Schulz and L. M. Sehgal

*Institute of Theoretical Physics, RWTH Aachen  
D-52056 Aachen, Germany*

## Abstract

We have studied in detail the spectrum of the decay  $\mu^- \rightarrow e^- \bar{\nu}_e \nu_\mu \gamma$  as a function of the electron helicity, and verify the prediction [1] that a significant fraction of the electrons in this decay is right-handed. These “wrong-helicity” electrons persist in the limit  $\lambda = m_e/m_\mu \rightarrow 0$ , and are connected with helicity-flip bremsstrahlung in QED. The longitudinal polarization of the electron is calculated as a function of the photon and electron energy, and deviates systematically from the naive V-A prediction  $P_L = -1$ . The right-handed component is concentrated in the collinear region  $\theta \lesssim m_e/E_e$ . In the limit  $\lambda \rightarrow 0$ , we reproduce the results obtained in [1] using the helicity-flip splitting function introduced by Falk and Sehgal.

## 1 Introduction

In a recent Letter [1] it was pointed out that as a consequence of helicity-flip bremsstrahlung, electrons in the radiative decay  $\mu^- \rightarrow e^- \bar{\nu}_e \nu_\mu \gamma$  are not purely left-handed, even in the limit  $m_e \rightarrow 0$ . The decay width into right-handed electrons was shown to be  $\Gamma_R = \frac{\alpha}{4\pi} \Gamma_0$ , where  $\Gamma_0 \equiv G_F^2 m_\mu^5 / (192\pi^3)$ . The energy spectrum of these wrong-helicity electrons was calculated, as also that of the photons accompanying them. These results were obtained using the helicity-flip splitting function  $D_{\text{hf}}(z) = \frac{\alpha}{4\pi} z$  introduced by Falk and Sehgal [2].

The appearance of right-handed electrons in  $\mu$ -decay is, at first sight, surprising since it goes against the conventional wisdom based on the V-A structure of weak interaction and the common assumption of helicity-conservation in massless QED. However persistence of helicity-flip bremsstrahlung in the  $m_e \rightarrow 0$  limit has been established in several calculations of radiative processes [3, 4, 5, 6, 7], going back to the seminal paper of Lee and Nauenberg [8]. In all cases, the origin of the effect is the characteristic behaviour of helicity-flip bremsstrahlung at small angles

$$d\sigma_{\text{hf}} \approx \left(\frac{m_e}{E_e}\right)^2 \frac{d\theta^2}{\left[\theta^2 + \left(\frac{m_e}{E_e}\right)^2\right]^2}, \quad (1)$$

leading to a non-zero integrated rate that survives the limit  $m_e \rightarrow 0$ .

In the present paper, we derive the helicity-dependent spectrum of the decay  $\mu^- \rightarrow e^- \bar{\nu}_e \nu_\mu \gamma$  from first principles, without neglecting the electron mass. We obtain the longitudinal polarization  $P_L$  of the electron as a function of the electron energy, photon energy and the angle between the electron and photon. We then consider the limit  $m_e \rightarrow 0$  to demonstrate that the deviation from  $P_L = -1$  is present even in the chiral limit of QED. The results are compared with those obtained in the equivalent particle approach based on the helicity-flip fragmentation function, thus providing a confirmation of the statements in Ref.[1].

## 2 Matrix Element and Phase Space for $\mu^- \rightarrow e^- \bar{\nu}_e \nu_\mu \gamma$

The matrix element for the decay  $\mu^- \rightarrow e^- \bar{\nu}_e \nu_\mu \gamma$  may be obtained from the Feynman diagrams shown in Fig.(1). Adopting the notation of Ref.[9, 10], the square of the matrix element, summed over the photon polarization, is

$$|\mathcal{M}|^2 \sim C^{\alpha\beta} N_{\alpha\beta}, \quad (2)$$

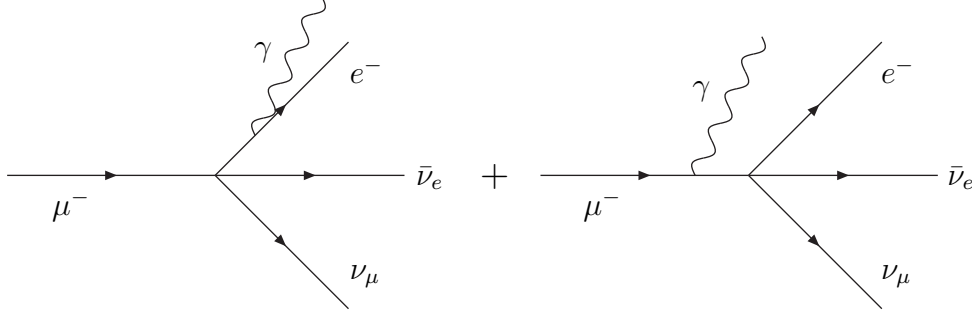


Figure 1: Feynman diagrams

where, in agreement with Ref. [9]

$$\begin{aligned}
C^{\alpha\beta} = \frac{e^2}{2(p_e \cdot k)^2 (p_\mu \cdot k)^2} \{ & (p_\mu \cdot k)^2 [(k \cdot \bar{p}_e - m_e^2) T_1^{\alpha\beta} + k \cdot \bar{p}_e T_3^{\alpha\beta} - m_e^2 T_7^{\alpha\beta}] \\
& + (p_e \cdot k)^2 [(k \cdot \bar{p}_\mu + m_\mu^2) T_2^{\alpha\beta} - k \cdot \bar{p}_\mu T_4^{\alpha\beta} - m_\mu^2 T_7^{\alpha\beta}] \\
& + (p_e \cdot k) (p_\mu \cdot k) [p_\mu \cdot \bar{p}_e T_1^{\alpha\beta} - p_e \cdot \bar{p}_\mu T_2^{\alpha\beta} + k \cdot \bar{p}_\mu T_5^{\alpha\beta} - k \cdot \bar{p}_e T_6^{\alpha\beta} + 2p_e \cdot p_\mu T_7^{\alpha\beta}] \}, \quad (3)
\end{aligned}$$

with

$$\begin{aligned}
T_1^{\alpha\beta} &:= (k^\alpha \bar{p}_\mu^\beta + k^\beta \bar{p}_\mu^\alpha - k \cdot \bar{p}_\mu g^{\alpha\beta}), & T_2^{\alpha\beta} &:= (k^\alpha \bar{p}_e^\beta + k^\beta \bar{p}_e^\alpha - k \cdot \bar{p}_e g^{\alpha\beta}), \\
T_3^{\alpha\beta} &:= (p_e^\alpha \bar{p}_\mu^\beta + p_e^\beta \bar{p}_\mu^\alpha - p_e \cdot \bar{p}_\mu g^{\alpha\beta}), & T_4^{\alpha\beta} &:= (p_\mu^\alpha \bar{p}_e^\beta + p_\mu^\beta \bar{p}_e^\alpha - p_\mu \cdot \bar{p}_e g^{\alpha\beta}), \\
T_5^{\alpha\beta} &:= (p_e^\alpha \bar{p}_e^\beta + p_e^\beta \bar{p}_e^\alpha - m_e^2 g^{\alpha\beta}), & T_6^{\alpha\beta} &:= (p_\mu^\alpha \bar{p}_\mu^\beta + p_\mu^\beta \bar{p}_\mu^\alpha - m_\mu^2 g^{\alpha\beta}), \\
T_7^{\alpha\beta} &:= (\bar{p}_e^\alpha \bar{p}_\mu^\beta + \bar{p}_e^\beta \bar{p}_\mu^\alpha - \bar{p}_e \cdot \bar{p}_\mu g^{\alpha\beta})
\end{aligned} \quad (4)$$

and

$$N_{\alpha\beta} = -Q^2 g_{\alpha\beta} + Q_\alpha Q_\beta. \quad (5)$$

Here  $Q = p_\mu - p_e - k$  denotes the total momentum carried away by the neutrino pair,  $p_\mu$ ,  $p_e$ ,  $k$  denoting the momenta of  $\mu$ ,  $e$  and  $\gamma$ . We have introduced the notation

$$\bar{p}_\mu = p_\mu - m_\mu s_\mu, \quad \bar{p}_e = p_e - m_e s_e. \quad (6)$$

For the purpose of the present investigation, we will consider unpolarized muons, thus omitting terms containing  $s_\mu$ . The spectrum will be obtained in terms of the invariants

$$x := \frac{2p_\mu \cdot p_e}{m_\mu^2}, \quad y := \frac{2p_\mu \cdot k}{m_\mu^2}, \quad z := \frac{2p_e \cdot k}{m_\mu^2} \quad (7)$$

and the mass ratio  $\lambda := m_e/m_\mu$ . In the rest frame of the muon,

$$x = \frac{2E_e}{m_\mu}, \quad y = \frac{2E_\gamma}{m_\mu}, \quad z = \frac{y}{2} [x - \cos(\theta) \sqrt{x^2 - 4\lambda^2}], \quad (8)$$

$E_e, E_\gamma$  being the energies of the electron, photon and  $\cos(\theta)$  the angle between them. The boundary of phase space is determined by the condition  $-1 \leq \cos(\theta) \leq 1$ , and  $0 \leq Q^2 \leq (1 - \lambda)^2 m_\mu^2$ ,  $Q^2$  being the ‘‘missing mass’’ of the neutrino pair. This leads to the condition

$$0 \leq y \leq y_m(x), \quad 2\lambda \leq x \leq 1 + \lambda^2, \quad (9)$$

where

$$y_m(x) = 2 \frac{1 + \lambda^2 - x}{2 - x + \sqrt{x^2 - 4\lambda^2}}. \quad (10)$$

Equivalently, the limits of phase space may be expressed as

$$2\lambda \leq x \leq x_m(y), \quad 0 \leq y \leq 1 - \lambda, \quad (11)$$

where

$$x_m(y) = \frac{\lambda^2 + (1-y)^2}{1-y}. \quad (12)$$

The differential decay width for  $\mu^- \rightarrow e^- \bar{\nu}_e \nu_\mu \gamma$  in the variables  $x$ ,  $y$  and  $\cos(\theta)$  is then given by

$$\left( \frac{d\Gamma}{dx dy d\cos(\theta)} \right)_{\text{R,L}} = (-1) \Gamma_0 \frac{\alpha}{2\pi} \sqrt{x^2 - 4\lambda^2} \frac{1}{y z^2} \frac{1}{2} (g_0 \pm g_1) \quad (13)$$

where R and L denote right-handed and left-handed electrons, corresponding to the polarization vectors

$$(s_e)_{\text{R}} = \left( \frac{|\mathbf{p}_e|}{m_e}, \frac{E_e}{m_e} \hat{\mathbf{p}}_e \right) \quad (s_e)_{\text{L}} = \left( \frac{|\mathbf{p}_e|}{m_e}, -\frac{E_e}{m_e} \hat{\mathbf{p}}_e \right). \quad (14)$$

The functions  $g_0$  and  $g_1$  are given by

$$\begin{aligned} g_0 := & -2xy z^2 + 6xy z^3 - 6x y^2 z - 8x y^2 z^2 + 6x y^3 z + 6x z^2 + 8x z^3 - 6x^2 y z - 8x^2 y z^2 \\ & + 8x^2 y^2 z - 4x^2 z^2 + 4x^3 y z + 6y z^2 + 5y z^3 - 2y z^4 - 2y^2 z^2 + 2y^2 z^3 - 3y^3 z - 2y^3 z^2 \\ & + 2y^4 z - 6z^3 - 4z^4 \\ & + \lambda^2 (8xyz + 6xy z^2 + 2x y^2 z + 6x y^2 - 8x y^3 + 6x z^2 - 6x^2 y z - 4x^2 y^2 + 6y z^2 - 3y z^3 \\ & \quad - 6y^2 z - 2y^2 z^2 + 5y^3 z + 6y^3 - 4y^4 - 8z^2 - 6z^3) \\ & + \lambda^4 (6xy^2 - 6y^2 z - 8y^2 + 6y^3), \end{aligned} \quad (15)$$

$$\begin{aligned} g_1 := & \{ 6x^3 y z - 4x^4 y z + 6x^2 y^2 z - 8x^3 y^2 z + 3x y^3 z - 6x^2 y^3 z - 2x y^4 z - 6x^2 z^2 + 4x^3 z^2 \\ & - 6x y z^2 + 2x^2 y z^2 + 8x^3 y z^2 + 2x y^2 z^2 + 8x^2 y^2 z^2 + 2x y^3 z^2 + 6x z^3 - 8x^2 z^3 \\ & - 5x y z^3 - 6x^2 y z^3 - 2x y^2 z^3 + 4x z^4 + 2x y z^4 \\ & + \lambda^2 (-6x^2 y^2 + 4x^3 y^2 - 6x y^3 + 8x^2 y^3 - 6y^4 + 8x y^4 - 24x y z + 16x^2 y z - 4y^2 z^3 \\ & \quad + 4y^5 + 2x^3 y z + 22x y^2 z - 6x^2 y^2 z + 4y^3 z - 7x y^3 z - 4y^4 z + 24z^2 - 16x z^2 - 2x^2 z^2 \\ & \quad - 16y z^2 - 18x y z^2 - 2x^2 y z^2 - 6y^2 z^2 + 10x y^2 z^2 + 4y^3 z^2 + 16z^3 + 2x z^3 + x y z^3) \\ & + \lambda^4 (24y^2 - 16x y^2 - 2x^2 y^2 - 16y^3 - 2x y^3 - 2y^4 - 8x y z + 16y^2 z + 2x y^2 z - 4y^3 z \\ & \quad + 8z^2 - 2y^2 z^2) \\ & + 8\lambda^6 y^2 \} \cdot \frac{1}{2\sqrt{x^2 - 4\lambda^2}}. \end{aligned} \quad (16)$$

Adding the expressions for  $d\Gamma_{\text{R}}$  and  $d\Gamma_{\text{L}}$ , we obtain the spectrum for unpolarized electrons, which depends on the function  $g_0$  only [10]. The specific effects of electron helicity are contained in the function  $g_1$ .

### 3 Unpolarized Spectra (summed over electron helicity)

Summing over the electron helicity, the differential decay rate of  $\mu^- \rightarrow e^- \bar{\nu}_e \nu_\mu \gamma$  is

$$\left( \frac{d\Gamma}{dx dy d\cos(\theta)} \right)_{\text{R+L}} = (-1) \Gamma_0 \frac{\alpha}{2\pi} \sqrt{x^2 - 4\lambda^2} \frac{1}{y z^2} g_0. \quad (17)$$

From this we can derive the following spectra.

### 3.1 Dalitz plot in electron and photon energies

$$\begin{aligned}
\left(\frac{d\Gamma}{dx dy}\right)_{\text{R+L}} &= (-1)\Gamma_0 \frac{\alpha}{2\pi} \int_{-1}^{+1} d\cos(\theta) \sqrt{x^2 - 4\lambda^2} \frac{1}{y z^2} g_0(x, y, z; \lambda) \\
&= \Gamma_0 \frac{\alpha}{6\pi} \frac{1}{y} \left( \mathcal{A} \{ 12y(-6 + 3y + y^2) + x(-72 + 78y + 33y^2 - 6y^3) \right. \\
&\quad + 2x^2(24 + 12y - 5y^2 + 2y^3) \\
&\quad + \lambda^2 [96 - 72y + 4y^2 - 4y^3 + 9x(-8 - 2y + y^2)] \} \\
&\quad + 12\mathcal{L} \{ -4x^3 + x^2(6 - 8y) + 6\lambda^4 y - 6x(-1 + y)y + (3 - 2y)y^2 \\
&\quad \left. + \lambda^2 [6x^2 + (6 - 5y)y - 2x(4 + y)] \} \right), \tag{18}
\end{aligned}$$

where we have defined

$$\mathcal{A} := \sqrt{x^2 - 4\lambda^2}, \quad \mathcal{L} := \frac{1}{2} \log\left(\frac{x + \mathcal{A}}{x - \mathcal{A}}\right). \tag{19}$$

### 3.2 Photon Energy Spectrum

The photon energy spectrum is given by

$$\begin{aligned}
\left(\frac{d\Gamma}{dy}\right)_{\text{R+L}} &= \int_{2\lambda}^{x_m(y)} dx \left(\frac{d\Gamma}{dx dy}\right)_{\text{R+L}} \\
&= \Gamma_0 \frac{\alpha}{36\pi} \frac{1}{y} \left\{ [(-102 + 46y - 95y^2 + 109y^3 - 45y^4 + 21y^5 - 6y^6)(1 - y) \right. \\
&\quad + 6\lambda^2(64 - 250y + 386y^2 - 240y^3 + 67y^4 - 20y^5 + 5y^6)(1 - y)^{-1} \\
&\quad + 18\lambda^4 y(18 + 12y - 40y^2 + 11y^3 + 3y^4)(1 - y)^{-2} \\
&\quad + 2\lambda^6(-192 + 622y - 856y^2 + 552y^3 - 105y^4 - 21y^5)(1 - y)^{-4} \\
&\quad + 3\lambda^8(34 - 64y - 13y^2 + 4y^3)(1 - y)^{-4}] \\
&\quad + [24(-3 + 2y - 4y^2 + 2y^3)(1 - y) + 72\lambda^2 y(-13 + 19y - 7y^2)(1 - y)^{-1} \\
&\quad + 72\lambda^4(12 - 27y + 18y^2 - 5y^3)(1 - y)^{-1} + 24\lambda^6 y(5 + 15y - 18y^2)(1 - y)^{-3} \\
&\quad \left. + 72\lambda^8(-1 + 2y)(1 - y)^{-4}] \log\left(\frac{\lambda}{1 - y}\right) \right\}. \tag{20}
\end{aligned}$$

The leading term for small  $y$  (small photon energies) is

$$\left(\frac{d\Gamma}{dy}\right)_{\text{R+L}} \xrightarrow{y \rightarrow 0} \Gamma_0 \frac{\alpha}{6\pi} \frac{1}{y} [(-17 + 64\lambda^2 - 64\lambda^6 + 17\lambda^8) + (-12 + 144\lambda^4 - 12\lambda^8) \log(\lambda)]. \tag{21}$$

In the limit of small  $\lambda$ , this reduces to the approximate form

$$\left(\frac{d\Gamma}{dy}\right)_{\text{R+L}} \xrightarrow{\lambda \rightarrow 0} \Gamma_0 \frac{\alpha}{6\pi} \frac{1}{y} [-17 - 12 \log(\lambda)], \tag{22}$$

which agrees with the old calculation of Eckstein and Pratt [11] and Kinoshita and Sirlin [12], in which terms of order  $\lambda^2$  and higher powers were neglected.

### 3.3 Electron energy spectrum

The result for the electron energy spectrum is as follows

$$\left(\frac{d\Gamma}{dx}\right)_{\text{R+L}} = \Gamma_0 \frac{\alpha}{\pi} \frac{1}{\mathcal{A}} u^{-4} (u^2 - \lambda^2) \left[ k_1 + \log\left(\frac{u}{\lambda}\right) k_2 + \log\left(\frac{1-u}{y_0}\right) k_3 + \log\left(\frac{u}{\lambda}\right) \log\left(\frac{1-u}{y_0}\right) k_4 \right], \quad (23)$$

where

$$\begin{aligned} k_1 &:= \frac{1}{36} (u^2 - \lambda^2) (1 - y_0 - u) \left[ u^2 (-300 + 399u + 71u^2 + 2u^3 + 8u^4 + 132y_0 + 63uy_0 - 10u^2y_0 \right. \\ &\quad \left. - 8u^3y_0 + 24y_0^2 - 12uy_0^2 + 8u^2y_0^2) \right. \\ &\quad \left. + \lambda^2 u (555 - 259u - 61u^2 - 19u^3 + 87y_0 - 28uy_0 + 19u^2y_0 \right. \\ &\quad \left. - 12y_0^2 + 8uy_0^2) \right. \\ &\quad \left. + \lambda^4 (122 - 67u - 19u^2 - 22y_0 + 19uy_0 + 8y_0^2) \right], \\ k_2 &:= \frac{1}{3} u (1 - y_0 - u) \left[ u^2 (5 + 17u - 34u^2 + 5y_0 - 14uy_0 - 4y_0^2) + 3\lambda^2 u (6 - 19u + u^2 - 6y_0 - 5uy_0) \right. \\ &\quad \left. + 12\lambda^4 (-4 - u + 3u^2) \right], \\ k_3 &:= 4(\lambda^2 - u^2) [u^3(3 - 2u) + \lambda^2 u(3 - 8u + 3u^2) + \lambda^4(-2 + 3u)], \\ k_4 &:= 4(\lambda^2 + u^2) [u^3(3 - 2u) + \lambda^2 u(3 - 8u + 3u^2) + \lambda^4(-2 + 3u)], \end{aligned} \quad (24)$$

where  $u = (x + \mathcal{A})/2$ . The normalized electron energy spectrum is shown in Fig.(2a). In the limit  $\lambda \rightarrow 0$  we

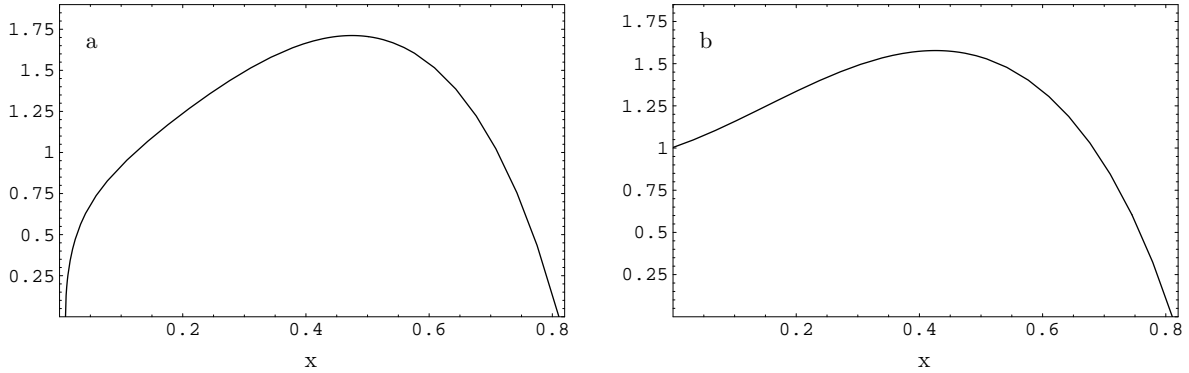


Figure 2: Normalized electron energy spectrum  $(\Gamma_{\text{R+L}})^{-1} \left(\frac{d\Gamma}{dx}\right)_{\text{R+L}}$  for  $y_0 \approx 0.189$  ( $E_{\gamma_0} = 10$  MeV) and a)  $\lambda = m_e/m_\mu \approx 1/207$ , b)  $\lambda \rightarrow 0$ .

have for the  $x$ -spectrum

$$\begin{aligned} \lim_{\lambda \rightarrow 0} (\Gamma_{\text{R+L}})^{-1} \left(\frac{d\Gamma}{dx}\right)_{\text{R+L}} &= \left\{ (1 - y_0 - x) [-5 - 5y_0 + 4y_0^2 + x(-17 + 14y_0) + 34x^2] \right. \\ &\quad \left. + 12x^2(-3 + 2x) \log\left(\frac{1-x}{y_0}\right) \right\} \\ &\quad \times \left[ (1 - y_0)(7 - 3y_0 + 3y_0^2 - y_0^3) + 6 \log(y_0) \right]^{-1}. \end{aligned} \quad (25)$$

This is shown in Fig.(2b).

In the limit  $y_0 \rightarrow 0$  we reproduce the spectrum for non-radiative muon decay

$$\lim_{\lambda \rightarrow 0, y_0 \rightarrow 0} (\Gamma_{R+L})^{-1} \left( \frac{d\Gamma}{dx} \right)_{R+L} = (\Gamma_{R+L})^{-1} \left( \frac{d\Gamma}{dx} \right)^{\text{non-rad}} = 2x^2(3-2x). \quad (26)$$

### 3.4 Unpolarized Rate for minimum photon energy

Integrating Eq.(20) in the interval  $y_0 < y < 1 - \lambda$ , we obtain

$$\Gamma_{R+L}(y_0) = \Gamma_0 \frac{\alpha}{\pi} \left\{ f_1 + f_5 \log\left(\frac{1-\lambda}{y_0}\right) + \log\left(\frac{\lambda}{1-y_0}\right) \left[ f_2 + f_4 \log\left(\frac{\lambda}{1-y_0}\right) + f_3 \log(y_0) \right] + f_3 [\text{Li}_2(\lambda) - \text{Li}_2(1-y_0)] \right\}, \quad (27)$$

with

$$\begin{aligned} f_1 := & \frac{1}{2520} (1-\lambda-y_0) \{ 13409 - 2831y_0 + 3364y_0^2 - 2236y_0^3 + 669y_0^4 - 255y_0^5 + 60y_0^6 \\ & + \lambda(1229 - 1602y_0 + 1762y_0^2 - 474y_0^3 + 195y_0^4 - 60y_0^5) \\ & + 2\lambda^2(-41823 + 20376y_0 - 2893y_0^2 + 510y_0^3 - 180y_0^4) \\ & + 2\lambda^3(-15293 + 20376y_0 - 2893y_0^2 + 510y_0^3 - 180y_0^4)(1-y_0)^{-1} \\ & + 2\lambda^4(-27263 + 34693y_0 - 8835y_0^2 - 450y_0^3)(1-y_0)^{-1} \\ & + 10\lambda^5(-7309 + 16104y_0 - 10562y_0^2 + 1677y_0^3 + 90y_0^4)(1-y_0)^{-3} \\ & + 5\lambda^6(5 - 260y_0 - 153y_0^2 + 408y_0^3)(1-y_0)^{-3} \\ & + 35\lambda^7(431 - 897y_0 + 372y_0^2)(1-y_0)^{-3} \}, \end{aligned} \quad (28)$$

$$\begin{aligned} f_2 := & -\frac{1}{6} \{ 2(1-y_0)(-7 + 3y_0 - 3y_0^2 + y_0^3) + 6\lambda^2(19 - 24y_0 + 7y_0^2) \\ & + 3\lambda^4(65 - 52y_0 + 10y_0^2) + \lambda^6(87 - 82y_0 - y_0^2)(1-y_0)^{-2} \\ & + \lambda^8(3 - 21y_0 + 39y_0^2 - 17y_0^3)(1-y_0)^{-3} \}, \end{aligned}$$

$$f_3 := 2(1 - 12\lambda^4 + \lambda^8),$$

$$f_4 := \lambda^2(1 + 2\lambda^2 + 6\lambda^4 + \lambda^6),$$

$$f_5 := \frac{1}{6}(-17 + 64\lambda^2 - 64\lambda^6 + 17\lambda^8).$$

In the limit of small  $y_0$  and small  $\lambda$  this reduces to

$$\Gamma_{R+L}(y_0; \lambda) \xrightarrow{\lambda \rightarrow 0, y_0 \rightarrow 0} \Gamma_0 \frac{\alpha}{\pi} \left[ \log(\lambda) \left( 2 \log(y_0) + \frac{7}{3} \right) + \frac{17}{6} \log(y_0) - \frac{\pi^2}{3} + \frac{13409}{2520} \right], \quad (29)$$

which agrees with Ref. [11], except in the constant (non-logarithmic) term, which was  $-\pi^2/6 + 601/144$  in the old calculation.

## 4 Spectra for Right- and Left-handed Electrons

The spectra when the final electron is polarized in the state R or L are obtained using Eq.(13). We will emphasize the case R, which is the one which behaves in an unexpected way in the  $\lambda \rightarrow 0$  limit [1, 9]. The corresponding spectra for the state L are obtained by subtraction from the unpolarized result L+R discussed in Sec.3.

## 4.1 Dalitz plot for R-Electrons

$$\begin{aligned}
\left(\frac{d\Gamma}{dx dy}\right)_R = & \Gamma_0 \frac{\alpha}{12\pi} \frac{1}{\mathcal{A}} \frac{1}{y} \{36 \mathcal{A}^2 y^2 + \mathcal{A}(36 y^2 - 60 x y^2 - 24 y^3) + 12 \mathcal{A} \lambda^4 (-8 + y^2) \\
& + \lambda^2 [-288 \mathcal{A} + 96 \mathcal{A}^2 + 192 \mathcal{A} x - 72 \mathcal{A}^2 x + 24 \mathcal{A} x^2 + 192 \mathcal{A} y \\
& - 72 \mathcal{A}^2 y + 72 \mathcal{A} x y - 18 \mathcal{A}^2 x y + 6 \mathcal{A} x^2 y + 48 \mathcal{A} y^2 + 4 \mathcal{A}^2 y^2 \\
& - 52 \mathcal{A} x y^2 + 9 \mathcal{A}^2 x y^2 - 3 \mathcal{A} x^2 y^2 - 24 \mathcal{A} y^3 - 4 \mathcal{A}^2 y^3 + 16 \mathcal{A} x y^3] \\
& + \mathcal{A}(\mathcal{A} - x) [-72 x + 48 x^2 - 72 y + 78 x y + 24 x^2 y + 33 x y^2 \\
& - 10 x^2 y^2 + 12 y^3 - 6 x y^3 + 4 x^2 y^3] \\
& + \mathcal{L} [-12(\mathcal{A} - x)(-3 + 2x + 2y)(2x^2 + 2xy + y^2) \\
& + \lambda^4(96x - 192y + 72\mathcal{A}y - 24xy + 48y^2) \\
& + \lambda^2(288x - 96\mathcal{A}x - 192x^2 + 72\mathcal{A}x^2 - 24x^3 + 72\mathcal{A}y - 264xy \\
& - 24\mathcal{A}xy + 72x^2y - 48y^2 - 60\mathcal{A}y^2 + 84xy^2 + 48y^3)] \}. \tag{30}
\end{aligned}$$

In the limit  $\lambda \rightarrow 0$  we obtain

$$\lim_{\lambda \rightarrow 0} \left(\frac{d\Gamma}{dx dy}\right)_R = \Gamma_0 \frac{\alpha}{\pi} y(3 - 2x - 2y). \tag{31}$$

This limiting result coincides with what one obtains on the basis of the helicity-flip splitting function. Denoting the electron spectrum in the non-radiative decay  $(d\Gamma/dx_0)^{\text{non-rad}}$ , the spectrum after helicity-flip bremsstrahlung is

$$\left(\frac{d\Gamma}{dx_0 dz}\right)_R = \left(\frac{d\Gamma}{dx_0}\right)^{\text{non-rad}} D_{\text{hf}}(z). \tag{32}$$

Noting that  $y = x_0 z$ ,  $x = x_0(1 - z)$ , and recalling that

$$\left(\frac{d\Gamma}{dx_0}\right)^{\text{non-rad}} = \Gamma_0 2x_0^2(3 - 2x_0), \quad D_{\text{hf}}(z) = \frac{\alpha}{2\pi} z, \tag{33}$$

we obtain

$$\left(\frac{d\Gamma}{dx dy}\right)_R = \frac{1}{x_0} \left(\frac{d\Gamma}{dx_0 dz}\right)_R = \Gamma_0 \frac{\alpha}{\pi} y(3 - 2x - 2y), \tag{34}$$

exactly as in Eq.(31).

## 4.2 Photon-Spectra for R- and L-electrons

Of particular interest is the photon energy spectrum associated with the right-handed polarization state of the electron, which is naively forbidden in the  $\lambda \rightarrow 0$  limit. The corresponding spectrum for L-electrons may be obtained by subtraction from Eq.(20). Our result is

$$\begin{aligned}
\left(\frac{d\Gamma}{dy}\right)_R &= \int_{2\lambda}^{x_m(y)} dx \left(\frac{d\Gamma}{dx dy}\right)_R \\
&= \Gamma_0 \frac{\alpha}{\pi} \left[ y(1 - y)(2 - y) + h_1 + \log\left(\frac{1 - y}{\lambda}\right) h_2 + \log^2\left(\frac{1 - y}{\lambda}\right) h_3 \right], \tag{35}
\end{aligned}$$

where

$$\begin{aligned}
h_1 &:= 4\lambda y(-3+2y) + \frac{1}{18}\lambda^2 \frac{1}{y} \frac{1}{1-y} (-248 + 176y + 489y^2 - 304y^3 - 53y^4 - 6y^5) \\
&\quad + \frac{8}{9}\lambda^3 \frac{1}{y} (48 - 10y + 15y^2 + 3y^3) + \frac{1}{4}\lambda^4 \frac{1}{y} \frac{1}{(1-y)^2} (-150 + 320y - 209y^2 + 16y^3 + 29y^4 - 2y^5) \\
&\quad + \frac{4}{9}\lambda^5 \frac{1}{y} (32 - 12y - 3y^2) + \frac{1}{18}\lambda^6 \frac{1}{y} \frac{1}{(1-y)^3} (-120 + 412y - 465y^2 + 114y^3 + 18y^4) \\
&\quad + \frac{1}{36}\lambda^8 \frac{1}{y} \frac{1}{(1-y)^4} (38 - 140y - 21y^2 + 6y^3), \\
h_2 &:= \frac{2}{3}\lambda^2 \frac{1}{y} \frac{1}{1-y} (8 + 13y - 30y^2 + 7y^3 + 5y^4) + \lambda^4 \frac{1}{y} \frac{1}{1-y} (-16 + 22y - 19y^2 + 3y^3) \\
&\quad + \frac{4}{3}\lambda^6 \frac{1}{(1-y)^3} (-1 - 6y + 6y^2) + \frac{2}{3}\lambda^8 \frac{1}{y} \frac{1}{(1-y)^4} (1 - 4y), \\
h_3 &:= 2\lambda^2(1-y)(-3-y) + 2\lambda^4 \frac{1}{y} (-2 - y + y^2).
\end{aligned} \tag{36}$$

In the limit  $m_e/m_\mu \rightarrow 0$  one obtains

$$\lim_{\lambda \rightarrow 0} \left( \frac{d\Gamma}{dy} \right)_R = \Gamma_0 \frac{\alpha}{\pi} y(1-y)(2-y), \tag{37}$$

which is the result derived in [1] on the basis of the helicity-flip fragmentation function  $D_{\text{hf}}(z)$ . The spectrum for  $\lambda \neq 0$  is plotted in Fig.(3). The striking feature is the appearance of a divergence at  $y = 0$ . This is

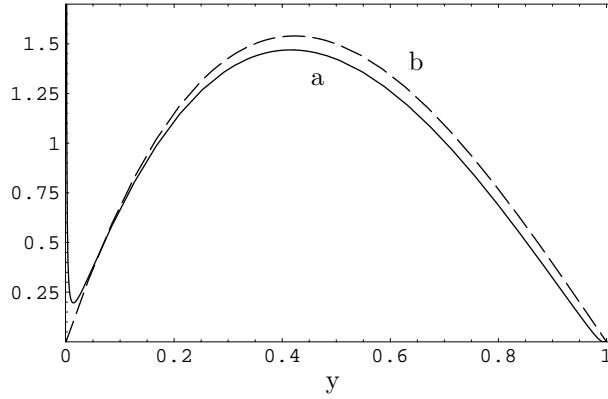


Figure 3: Photon energy spectrum  $\left( \frac{d\Gamma}{dy} \right)_R$  for right-handed electrons in units of  $\Gamma_0 \frac{\alpha}{4\pi}$  for a)  $\lambda = 1/207$ , b)  $\lambda \rightarrow 0$ .

connected with the fact that for  $m_e \neq 0$ , helicity is not a good quantum number. As a consequence, ordinary (non-flip) bremsstrahlung, diverging as  $1/y$  at small  $y$ , is partly transmitted to the final state with electron polarization  $s_e = s_e^R$ . This contribution vanishes in the limit  $\lambda \rightarrow 0$ , leaving behind the anomalous (helicity-flip) contribution in Eq.(37). This anomalous bremsstrahlung integrates to a decay width

$$\Gamma_R = \Gamma_0 \frac{\alpha}{4\pi} (1 - y_0) (1 + y_0 - 3y_0^2 + y_0^3), \tag{38}$$

which is the contribution of right-handed electrons to the muon decay width in the  $\lambda \rightarrow 0$  limit [1].

### 4.3 Decay Rates for R- and L-electrons, for minimum Photon Energy ( $y > y_0$ )

By integrating  $(d\Gamma/dy)_{R,L}$  in the interval  $y_0 \leq y \leq 1 - \lambda$ , we have obtained analytic results for the decay rates into right-handed and left-handed electrons.

$$\begin{aligned} \Gamma_R(y_0) = \Gamma_0 \frac{\alpha}{4\pi} \left\{ (1 - \lambda - y_0) (1 + y_0 - 3y_0^2 + y_0^3 + \lambda l_1) \right. \\ \left. + \lambda^2 \left[ \log\left(\frac{1-\lambda}{y_0}\right) l_2 + \log^2\left(\frac{1-y_0}{\lambda}\right) l_3 + \log\left(\frac{1-y_0}{\lambda}\right) l_4 \right. \right. \\ \left. \left. + (\text{Li}_2(\lambda) - \text{Li}_2(1-y_0)) l_5 + (\text{Li}_3(\lambda) - \text{Li}_3(1-y_0)) l_6 \right] \right\}, \end{aligned} \quad (39)$$

where

$$\begin{aligned} l_1 &:= \frac{1}{18} (1 - y_0)^{-3} \left[ -222 + 462 y_0 + 120 y_0^2 - 912 y_0^3 + 726 y_0^4 - 174 y_0^5 \right. \\ &\quad \left. + \lambda (-82 + 1216 y_0 - 3034 y_0^2 + 2632 y_0^3 - 622 y_0^4 - 104 y_0^5 - 6 y_0^6) \right. \\ &\quad \left. + \lambda^2 (-1122 + 3854 y_0 - 4700 y_0^2 + 2268 y_0^3 - 242 y_0^4 - 58 y_0^5) \right. \\ &\quad \left. + \lambda^3 (-169 + 646 y_0 - 1042 y_0^2 + 834 y_0^3 - 281 y_0^4 + 12 y_0^5) \right. \\ &\quad \left. + \lambda^4 (-1189 + 2901 y_0 - 2305 y_0^2 + 557 y_0^3 + 36 y_0^4) \right. \\ &\quad \left. + \lambda^5 (-71 + 84 y_0 - 49 y_0^2 + 36 y_0^3) + \lambda^6 (101 - 331 y_0 + 136 y_0^2) \right], \\ l_2 &:= \frac{2}{9} (-248 + 768 \lambda - 675 \lambda^2 + 256 \lambda^3 - 120 \lambda^4 + 19 \lambda^6), \\ l_3 &:= \frac{4}{3} \left[ (-7 + 18 y_0 - 6 y_0^2 - 2 y_0^3) + \lambda^2 (-18 + 6 y_0 - 3 y_0^2) + 12 \lambda^4 + \lambda^6 + 12 \lambda^2 \log(y_0) \right], \\ l_4 &:= \frac{2}{9} (1 - y_0)^{-3} \left[ (242 - 1062 y_0 + 1854 y_0^2 - 1582 y_0^3 + 612 y_0^4 - 36 y_0^5 - 28 y_0^6) \right. \\ &\quad \left. + \lambda^2 (45 - 459 y_0 + 1152 y_0^2 - 1152 y_0^3 + 459 y_0^4 - 45 y_0^5) \right. \\ &\quad \left. + \lambda^4 (204 - 444 y_0 + 288 y_0^2 - 48 y_0^3) \right. \\ &\quad \left. + \lambda^6 (13 - 27 y_0 + 45 y_0^2 - 19 y_0^3) \right. \\ &\quad \left. + 12 (1 - y_0)^3 \left\{ (8 - 24 \lambda^2 + \lambda^6) \log(y_0) - 12 \lambda^2 \text{Li}_2(1 - y_0) \right\} \right], \\ l_5 &:= \frac{8}{3} (8 - 24 \lambda^2 + \lambda^6), \quad l_6 := 32 \lambda^2. \end{aligned} \quad (40)$$

The functions  $\Gamma_R(y_0)$  and  $\Gamma_L(y_0)$  are plotted in Fig(4). The longitudinal polarization of the electron, defined as

$$P_L(y_0) := \frac{\Gamma_R(y_0) - \Gamma_L(y_0)}{\Gamma_R(y_0) + \Gamma_L(y_0)} \quad (41)$$

is plotted in Fig.(5). This figure demonstrates the presence of a significant right-handed electron component in radiative muon decay, which becomes as probable as the left-handed component at high photon energies. To illustrate the approach to the chiral limit  $\lambda \rightarrow 0$ , we have also shown in Fig.(5) the polarization of the electron in the decay  $\tau^- \rightarrow e^- \bar{\nu}_e \nu_\tau \gamma$ . In the chiral limit  $\lambda \rightarrow 0$  the longitudinal polarization goes from  $P_L = -1$  to  $P_L = 0$  like a step-function at  $y_0 = 1$ .

### 4.4 Electron Energy Spectra (R versus L), for given $y_0$

We have calculated the electron energy spectrum  $(d\Gamma/dx)_R$  for fixed  $y_0$ . The result is

$$\left( \frac{d\Gamma}{dx} \right)_R = \Gamma_0 \frac{\alpha}{\pi} \left[ j_1 + \log\left(\frac{u}{\lambda}\right) j_2 + \log\left(\frac{1-u}{y_0}\right) j_3 + \log\left(\frac{u}{\lambda}\right) \log\left(\frac{1-u}{y_0}\right) j_4 \right], \quad (42)$$

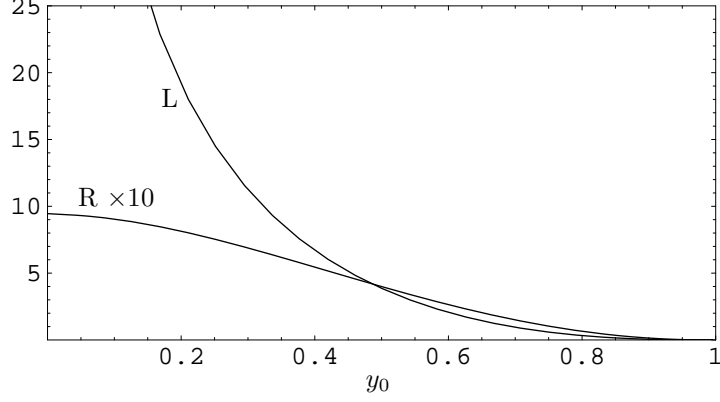


Figure 4: Integrated rates for R- and L-electrons  $\Gamma_{R,L}(y_0)$  in units of  $\Gamma_0 \frac{\alpha}{4\pi}$  as function of minimum photon energy  $y_0$ .

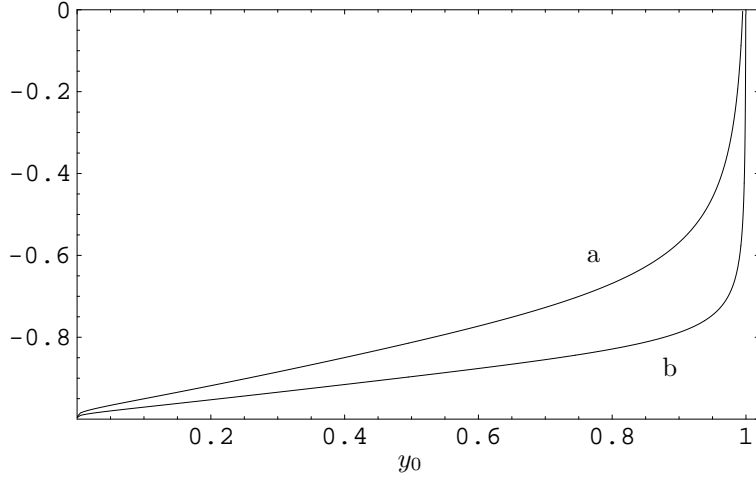


Figure 5: Longitudinal polarization of electron  $P_L$  as function of minimum photon energy  $y_0$ : a)  $\mu \rightarrow e$  decay, b)  $\tau \rightarrow e$  decay.

where

$$\begin{aligned}
 j_1 := & \frac{1}{36} \frac{1}{u^3} (1 - y_0 - u) \left\{ u^3 [30 + 12 u^2 + u (-42 - 12 y_0) + 30 y_0 - 24 y_0^2] \right. \\
 & + \lambda^2 u^2 [264 - 168 y_0 - 24 y_0^2 + u (261 - 15 y_0 - 12 y_0^2) \\
 & \quad \left. + u^2 (-155 - 26 y_0 + 4 y_0^2) + u^3 (-5 + 5 y_0) + u^4 (-5)] \right. \\
 & + \lambda^4 u [-555 - 87 y_0 + 12 y_0^2 + u (199 - 32 y_0 + 4 y_0^2) \\
 & \quad \left. + u^2 (73 + 5 y_0) + u^3 (-5)] \right. \\
 & \left. + \lambda^6 [-122 + 22 y_0 - 8 y_0^2 + 10 u (4 - y_0) + 10 u^2] \right\}, \tag{43}
 \end{aligned}$$

$$\begin{aligned}
j_2 &:= \frac{1}{3} \frac{1}{u^2} \frac{\lambda^2}{u^2 - \lambda^2} \left\{ u^2 (1 - y_0 - u) \left[ -5 - 5y_0 + 4y_0^2 + u(-19 + 12y_0 + 4y_0^2) + u^2(-13 - y_0) + 13u^3 \right] \right. \\
&\quad + 6\lambda^2 u (1 - y_0 - u) \left[ -3 + 3y_0 + u(2 + 3y_0) + u^2(-4 + y_0) + u^3 \right] \\
&\quad \left. + 24\lambda^4 (2 - u)(1 + u)(1 - y_0 - u) \right\}, \\
j_3 &:= 4 \frac{1}{u^3} \lambda^2 (1 - u) (\lambda^2 - u^2) (-2\lambda^2 + 3u - u^2), \\
j_4 &:= 4 \frac{1}{u^3} \lambda^2 (1 - u) (\lambda^2 + u^2) (-2\lambda^2 + 3u - u^2).
\end{aligned} \tag{44}$$

We have verified that in the limit  $\lambda \rightarrow 0$ , the right-handed spectrum takes the form

$$\left( \frac{d\Gamma}{dx} \right)_R \xrightarrow{\lambda \rightarrow 0} \Gamma_0 \frac{\alpha}{6\pi} (1 - y_0 - x) [5 + 5y_0 - 4y_0^2 + x(-7 - 2y_0) + 2x^2], \tag{45}$$

which is exactly the result derived in Ref.[1] on the basis of the fragmentation function  $D_{\text{hf}}(z)$ .

## 5 Discussion of the Collinear Region

A question of interest is the behaviour of helicity-flip and helicity-non-flip bremsstrahlung in the collinear region,  $\theta \approx 0$ , where  $\theta$  is the angle between the photon and electron in the final state. To this end, we have calculated exactly the distribution  $(d\Gamma/d\cos(\theta))_{\text{R,L}}$ . The analytic results are, however, too lengthy to be written down here. The left- and right-handed spectra for  $\lambda = 1/207$ , in the small angle region, are plotted in Fig.(6). The longitudinal polarization of the electron as a function of  $\theta$  is shown in Fig.(7), and, changes

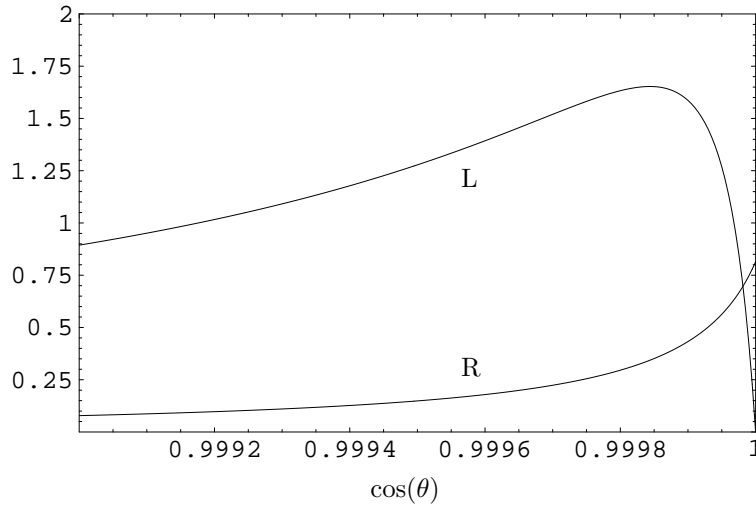


Figure 6:  $\cos(\theta)$  spectrum  $\left( \frac{d\Gamma}{d\cos(\theta)} \right)_{\text{L,R}}$  for  $\lambda = 1/207$  and  $y_0 = 0.189$  in units of  $\Gamma_0$ .

from the V-A value  $P_L \approx -1$  to the value  $P_L \approx +1$  in the forward direction. From the exact expressions we have derived the behaviour in the chiral limit  $\lambda \rightarrow 0$ . For  $\theta \neq 0$  and  $\lambda \rightarrow 0$ , we find

$$\begin{aligned}
\left( \frac{d\Gamma}{d\cos(\theta)} \right)_R &\xrightarrow{\lambda \rightarrow 0} \Gamma_0 \frac{\alpha}{6\pi} \pi \lambda \frac{1}{\theta^3} (1 - y_0) (5 + 5y_0 - 4y_0^2), \\
\left( \frac{d\Gamma}{d\cos(\theta)} \right)_L &\xrightarrow{\lambda \rightarrow 0} \Gamma_0 \frac{\alpha}{3\pi} \frac{1}{\theta^2} [-7 + 10y_0 - 6y_0^2 + 4y_0^3 - y_0^4 - 6\log(y_0)].
\end{aligned} \tag{46}$$

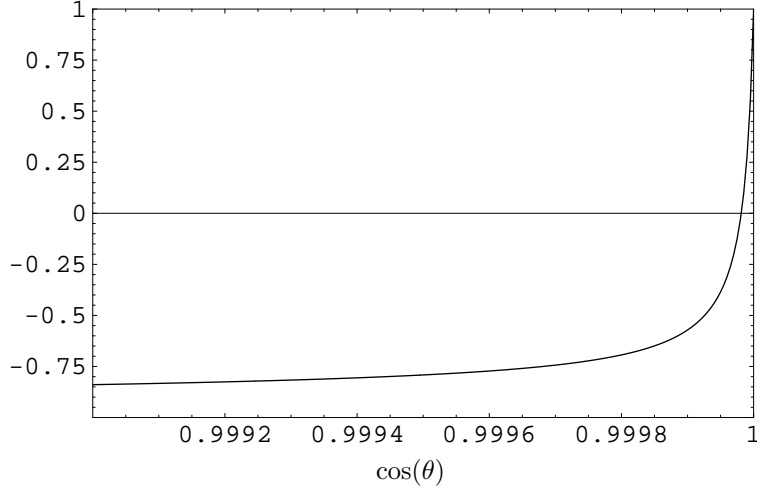


Figure 7: Longitudinal polarization  $P_L$  for  $\lambda = 1/207$  and  $y_0 = 0.189$ .

Note that, in the chiral limit, the  $\lambda/\theta^3$  behaviour of  $(d\Gamma/d \cos(\theta))_R$  refers to the opening angle of the electron and photon in the final state. The corresponding  $\lambda^2/\theta^4$  behaviour of the helicity-flip scattering cross section (Eq.(1)) refers to the angle between the photon and the incident electron.

We have also derived from the exact expressions the limits of  $(d\Gamma/d \cos(\theta))_{L,R}$  in the forward direction ( $\theta \rightarrow 0, \lambda \neq 0$ ). The results are

$$\begin{aligned}
\left(\frac{d\Gamma}{d \cos(\theta)}\right)_R \Big|_{\theta=0} &= \Gamma_0 \frac{\alpha}{\pi} \left\{ \frac{1}{360} \frac{1}{\lambda^2 (\zeta + \lambda)^2} [\zeta (180 \lambda^5 - 360 \lambda^6 - 180 \lambda^7 - 480 \lambda^8 + 240 \lambda^9 - 120 \lambda^{10}) \right. \\
&\quad + \zeta^2 (270 \lambda^4 - 900 \lambda^5 - 630 \lambda^6 - 720 \lambda^7 + 1440 \lambda^8 - 540 \lambda^9) \\
&\quad + \zeta^3 (60 \lambda^3 - 660 \lambda^4 - 780 \lambda^5 + 560 \lambda^6 + 2240 \lambda^7 - 940 \lambda^8) \\
&\quad + \zeta^4 (45 \lambda^2 - 270 \lambda^3 - 195 \lambda^4 + 1300 \lambda^5 + 1150 \lambda^6 - 770 \lambda^7) \\
&\quad + \zeta^5 (90 \lambda - 186 \lambda^2 + 120 \lambda^3 + 572 \lambda^4 + 50 \lambda^5 - 250 \lambda^6) \\
&\quad + \zeta^6 (15 - 42 \lambda - 20 \lambda^2 + 84 \lambda^3 - 45 \lambda^4) \\
&\quad + \zeta^7 (-6 - 40 \lambda + 12 \lambda^2) - 5 \zeta^8] \\
&\quad + \frac{1}{6} \log \left(1 + \frac{\zeta}{\lambda}\right) [\lambda^2 (-3 + 6 \lambda + 3 \lambda^2 + 8 \lambda^3 - 4 \lambda^4 + 2 \lambda^5) \\
&\quad + \zeta \lambda^2 (6 + 6 \lambda - 18 \lambda^3 + 6 \lambda^4) + \zeta^2 \lambda^2 (3 - 12 \lambda - 9 \lambda^2 + 6 \lambda^3) \\
&\quad + \zeta^3 \lambda^2 (-4 + 2 \lambda^2)] \left. \right\}, \tag{47}
\end{aligned}$$

$$\begin{aligned}
\left(\frac{d\Gamma}{d\cos(\theta)}\right)_L\Big|_{\theta=0} &= \Gamma_0 \frac{\alpha}{\pi} \frac{1}{120} \left\{ \frac{1}{(\zeta + \lambda)^2} [\zeta \lambda^5 (60 - 240\lambda + 60\lambda^2) + \zeta^2 \lambda^4 (90 - 600\lambda + 330\lambda^2) \right. \\
&\quad + \zeta^3 \lambda^3 (20 - 440\lambda + 500\lambda^2) + \zeta^4 \lambda^2 (15 - 120\lambda + 315\lambda^2 - 20\lambda^3) \\
&\quad + \zeta^5 \lambda (30 - 64\lambda + 90\lambda^2 - 20\lambda^3) + \zeta^6 (5 - 28\lambda + 15\lambda^2) - 4\zeta^7] \\
&\quad \left. + 60 \log\left(1 + \frac{\zeta}{\lambda}\right) \lambda^4 [1 + \lambda^2 - 2(\zeta + \lambda - 1)^2] \right\}, \tag{48}
\end{aligned}$$

where  $\zeta := 1 - y_0 - \lambda$ . For small  $\lambda$ , these collinear limits are

$$\begin{aligned}
\left(\frac{d\Gamma}{d\cos(\theta)}\right)_R\Big|_{\theta=0} &= \Gamma_0 \frac{\alpha}{\pi} \frac{1}{360} \frac{1}{\lambda^2} (1 - y_0)^4 (4 + 16y_0 - 5y_0^2) \\
\left(\frac{d\Gamma}{d\cos(\theta)}\right)_L\Big|_{\theta=0} &= \Gamma_0 \frac{\alpha}{\pi} \frac{1}{120} (1 - y_0)^4 (1 + 4y_0). \tag{49}
\end{aligned}$$

We have found that the angular distribution  $(d\Gamma/d\cos(\theta))_R$  connected with helicity-flip bremsstrahlung can be simulated by the following ansatz for the differential decay spectrum (where the label ‘‘APP’’ connotes ‘‘approximate’’):

$$\left(\frac{d\Gamma}{dx dy d\cos(\theta)}\right)_R^{\text{APP}} = \Gamma_0 \frac{2\alpha}{\pi} \lambda^2 y (3 - 2x - 2y) \frac{1}{(x - \cos(\theta) \mathcal{A})^2}. \tag{50}$$

When integrated over  $\cos(\theta)$ , this spectrum, in the limit  $\lambda \rightarrow 0$ , yields the Dalitz pair distribution given in Eq.(31). After integration over  $x$  and  $y$  we obtain an angular distribution  $(d\Gamma/d\cos(\theta))_R^{\text{APP}}$  which agrees with the exact calculation over a wide range of angles. This formula is particularly simple for  $y_0 = 0$ :

$$\left(\frac{d\Gamma(y_0 = 0)}{d\cos(\theta)}\right)_R^{\text{APP}} \xrightarrow{\lambda \rightarrow 0} \Gamma_0 \frac{\alpha}{\pi} \frac{5}{6} \lambda \left[1 + (\pi - \theta) \frac{\cos(\theta)}{\sin(\theta)}\right] \frac{1}{\sin^2(\theta)}, \tag{51}$$

which agrees with the small angle result given in Eq.(46). Similarly, in the forward direction ( $\theta = 0$ ), for small values of  $\lambda$ , the approximate representation Eq.(50) reproduces the result given in Eq.(49).

## 6 Conclusions

The purpose of this paper was to examine the dependence of the radiative decay  $\mu^- \rightarrow e^- \bar{\nu}_e \nu_\mu \gamma$  on the helicity of the final electron, in order to demonstrate the presence of right-handed electrons, even in the chiral limit  $m_e \rightarrow 0$ . This non-intuitive feature is a consequence of helicity-flip bremsstrahlung in QED, and was discussed in [1] with the help of the helicity-flip splitting function derived in [2]. We have now calculated the complete helicity-dependent spectrum of this decay from first principles, without neglecting the electron mass, and have shown that the results of [1] are reproduced in the limit  $\lambda \rightarrow 0$ . The presence of right-handed electrons manifests itself in the longitudinal polarization  $P_L = (\Gamma_R - \Gamma_L)/(\Gamma_R + \Gamma_L)$  which deviates from the naive V-A value  $P_L = -1$  even in the limit  $\lambda \rightarrow 0$ . The dependence of the polarization on the photon energy cut  $y_0$ , Fig.(5), shows that right-handed electrons occur predominantly with high energy photons. A characteristic signature of wrong-helicity electrons is also present in the opening-angle distribution  $d\Gamma/d\cos(\theta)$ , where the collinear region  $\theta \lesssim \lambda/(1 - y_0)$  is dominated by right-handed electrons. The fact that helicity-flip bremsstrahlung in the chiral limit  $m_e \rightarrow 0$  can be exactly reproduced by the simple and universal splitting function  $D_{\text{hf}}(z)$  in many different processes, is suggestive of a relationship to the chiral anomaly in QED [13, 14, 15].

## References

- [1] L. M. Sehgal, Phys. Lett. B **569**, 25 (2003).
- [2] B. Falk and L. M. Sehgal, Phys. Lett. B **325**, 509 (1994).
- [3] H. F. Contopanagos and M. B. Einhorn, Nucl. Phys. B **377**, 20 (1992).
- [4] S. Jadach, J. H. Kühn, R. G. Stuart and Z. Was, Z. Phys. C **38**, 609 (1988) [Erratum-ibid. C **45**, 528 (1990)].
- [5] L. Trentadue and M. Verbeni, Phys. Lett. B **478**, 137 (2000) and Nucl. Phys. B **583**, 307 (2000); A. V. Smilga, Comments Nucl. Part. Phys. **20**, 69 (1991).
- [6] S. Groote, J. G. Körner and M. M. Tung, Z. Phys. C **70**, 281 (1996).
- [7] W. E. Fischer and F. Scheck, Nucl. Phys. B **83**, 25 (1974).
- [8] T. D. Lee and M. Nauenberg, Phys. Rev. **133**, B1549 (1964).
- [9] M. Fischer, S. Groote, J. G. Körner and M. C. Mauser, Phys. Rev. D **67**, 113008 (2003).
- [10] A. Fischer, T. Kurosu and F. Savatier, Phys. Rev. D **49**, 3426 (1994).
- [11] S. G. Eckstein and R. R. Pratt, Ann. Phys. **8**, 297 (1959).
- [12] T. Kinoshita and A. Sirlin, Phys. Rev. **113**, 1652 (1959).
- [13] A. D. Dolgov and V. I. Zakharov, Nucl. Phys. B **27**, 525 (1971); K. Huang, *Quarks, Leptons And Gauge Fields* (World Scientific, Singapore, 1992); J. Horejsi, Czech. J. Phys. **42**, 241 (1992).
- [14] A. Freund and L. M. Sehgal, Phys. Lett. B **341**, 90 (1994).
- [15] R. D. Carlitz, J. C. Collins and A. H. Mueller, Phys. Lett. B **214**, 229 (1988).